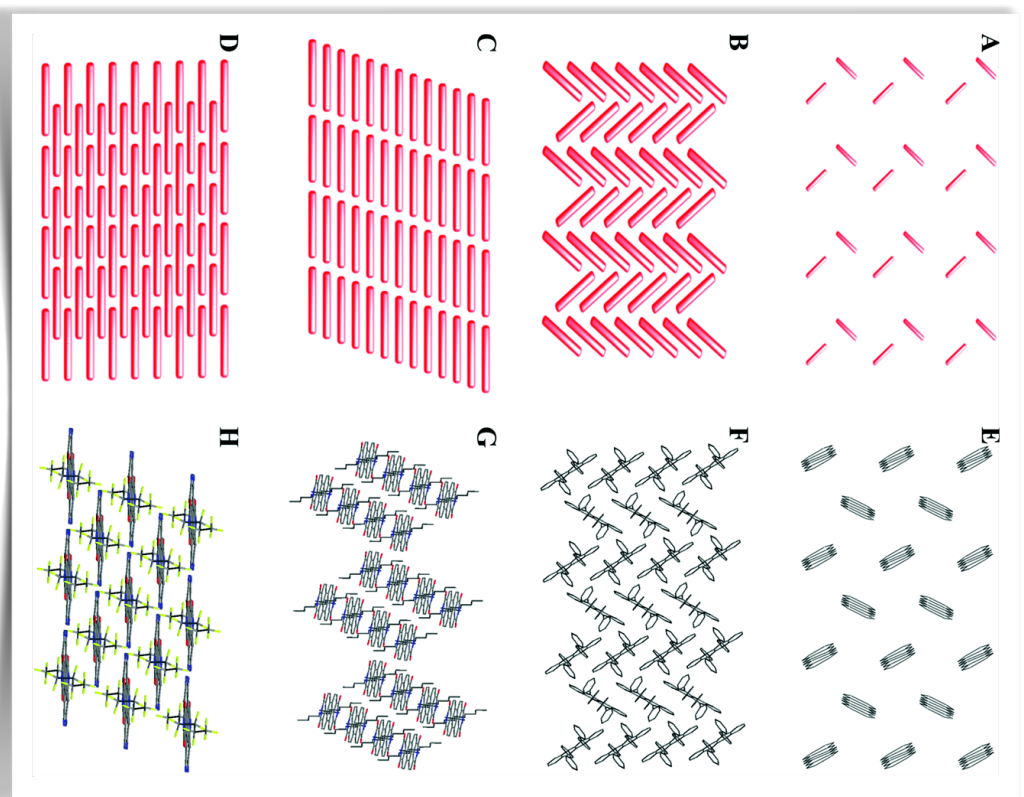


Self-energy embedding theory with coupled cluster Green's Function solver

Quantum embedding theory

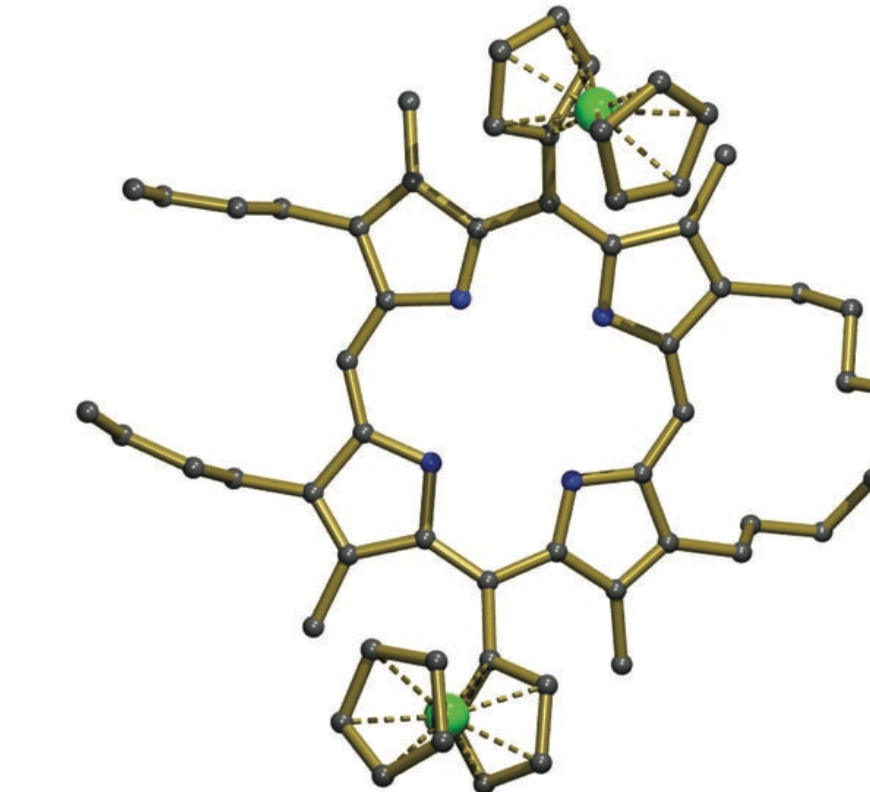
Material

- A single framework for different correlation strength (U): strong correlation, Mott etc.
- We want to use embedding theory for a class of materials which is not strongly correlated, but still requires very accurate modeling of correlation.



We will analyze real materials for various aspects of an embedding theory.

Molecule



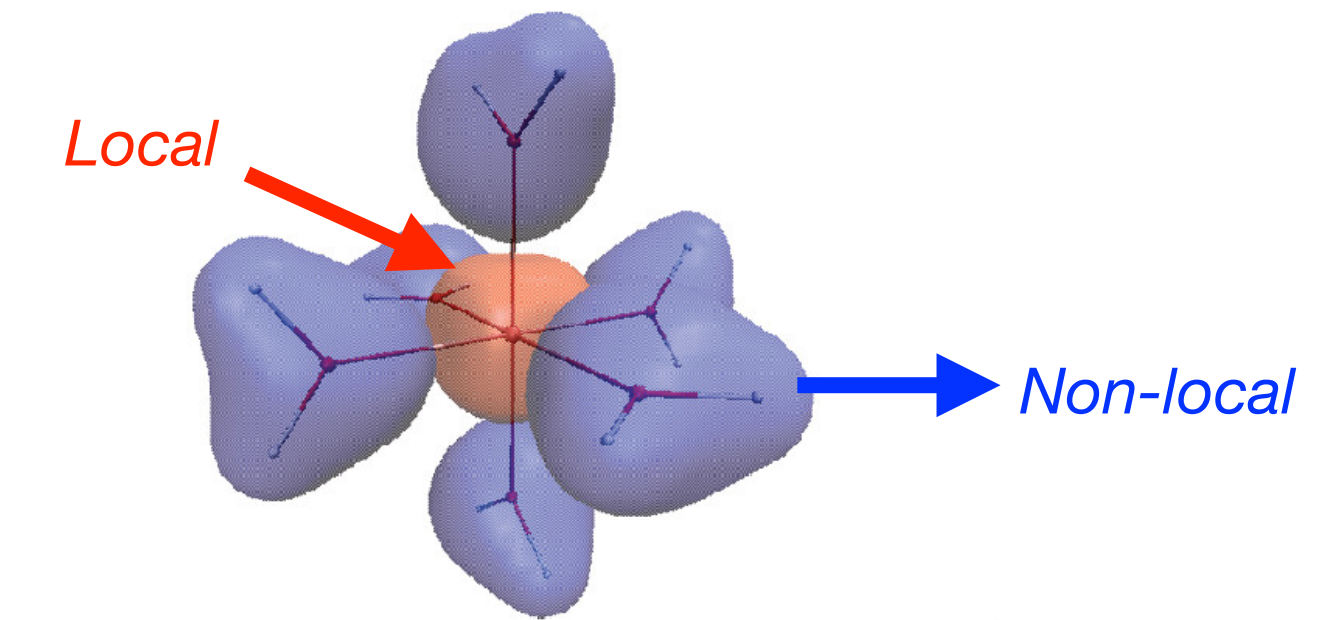
- Chemistry often demands accurate energetics. For a finite non-periodic system it is hard to reach convergence..
- However, small molecular systems can be a testbed for such theories.
- Perhaps embedding theory is better suited for spectra, local magnetic moments etc.

SEET in brief

- The basic framework of finite-temperature theories is provided by the Luttinger-Ward (LW) functional based definition of Ω , given by

$$\Omega = \Phi[G] - \text{Tr}(\log G^{-1}) - \text{Tr}\Sigma G$$

Skeleton diagrams in terms of G and bare interaction V



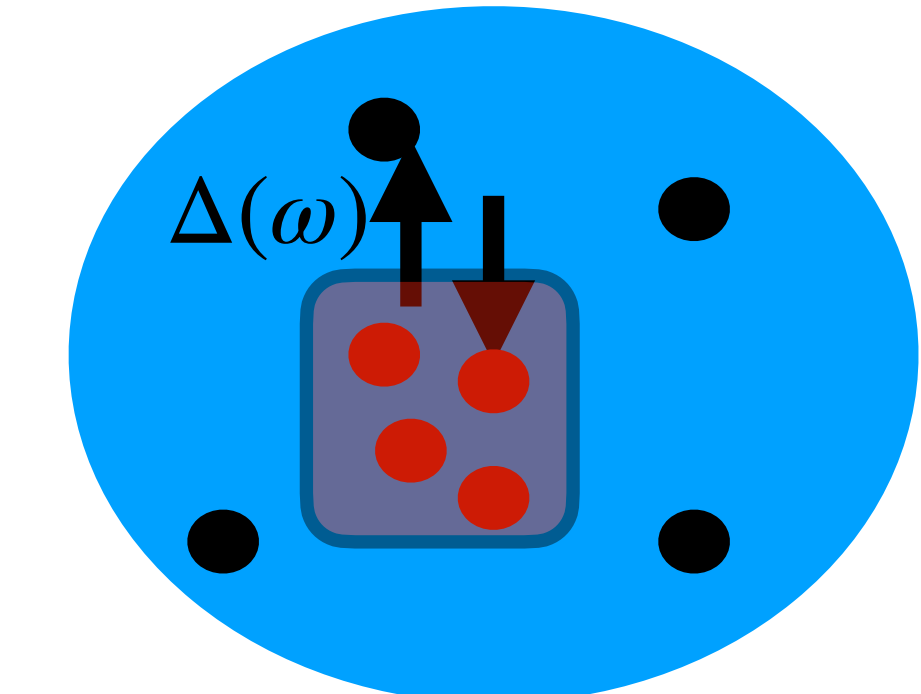
- $\Phi^{SEET} \approx \Phi_{non-loc}^{total} + \Phi_{loc}^{imp} - \Phi_{non-loc}^{imp}$

GW or GF2

Typically by exact solvers like ED or CT-QMC

$$\hat{H}_{imp} = \sum_{u,v} \tilde{F}_{uv} u^\dagger v + \sum_b \epsilon_b b^\dagger b + \sum_{u,b} V_{ub} (u^\dagger b + h.c.) + \frac{1}{2} \sum_{uvtw} v_{uvtw} u^\dagger v^\dagger w t$$

$$\tilde{F} = F_{loc} - \Sigma_{\infty, DC}$$



SEET vs GW+DMFT

SEET should be contrasted with GW+(E)DMFT (Kotliar, Biermann, Werner and many others) which uses ‘screened interaction’ W

$$\Psi^{GW+DMFT} = \Psi_{GW}^{total} + \Psi_{ED}^{imp}(G_{imp}, W) - \Psi_{GW}^{imp}(G_{imp}, W)$$

Embedding condition: $G_{loc}^{GW+DMFT} = G_{imp}$

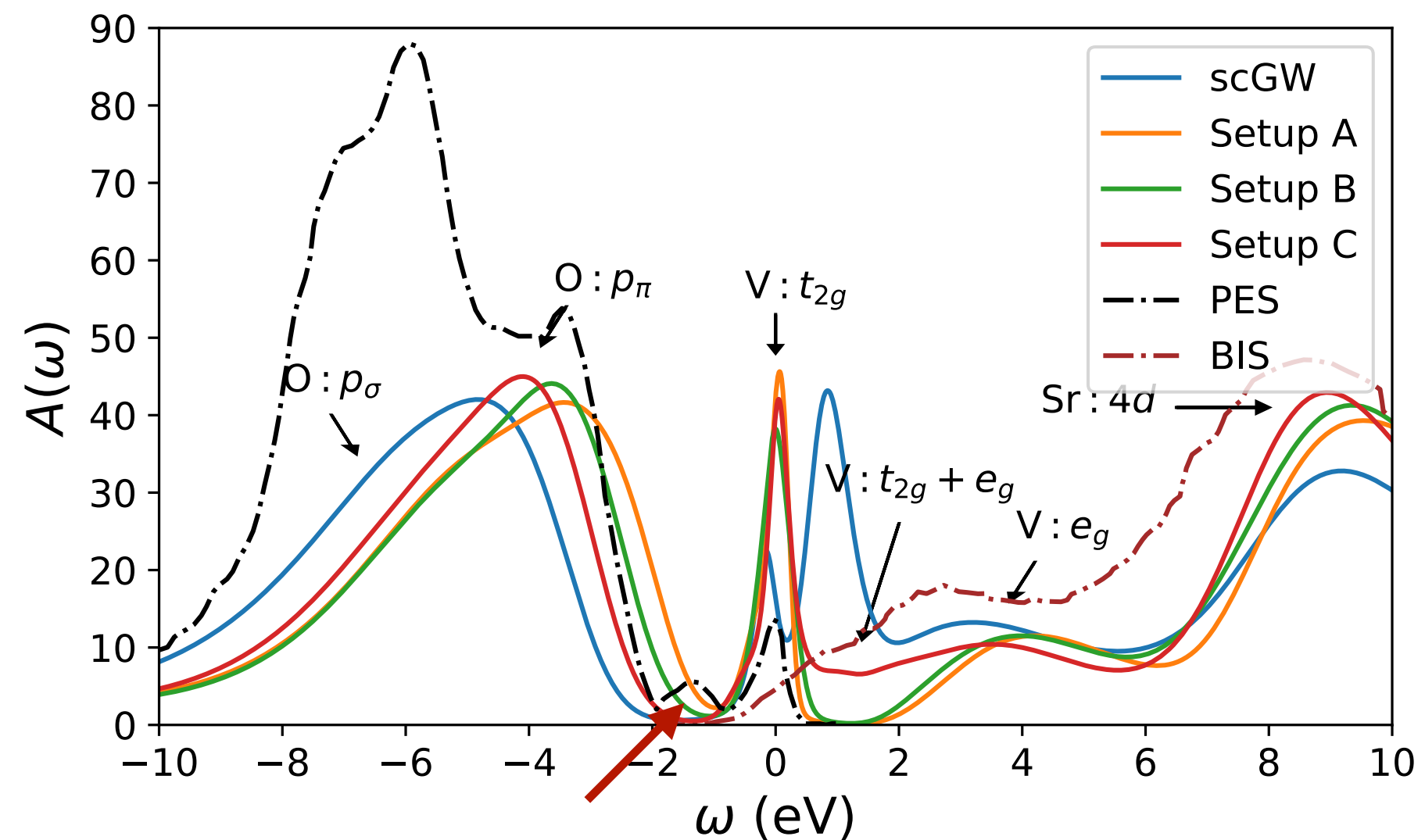
$$[G_{loc}^{SEET}]^{-1} = [G_0^{imp}]^{-1} - \tilde{\Sigma}_{non-loc}^{GW}; \tilde{\Sigma}_{non-loc}^{GW} = \Sigma_{loc}^{GW} - \Sigma_{DC}^{GW}$$

Hybridization: $\Delta^{SEET} = [G^{-1}]_{uv} - [G_{uv}]^{-1}$

$$\Delta^{GW+DMFT} = \Delta^{SEET}(\omega) - \Sigma_{loc}^{GW}(\omega) + \Sigma_{DC}^{GW}(\omega)$$

Consideration of bare V has the advantage of using “quantum chemistry” methods as solvers.

Impurity solver other than ED?



Satellite near E_{Fermi} was not reproduced

SrVO₃

C-N Yeh, S. Iskakov, D. Zgid, E. Gull, PRB 103 (19), 195149

Choice of impurities:

Name	Imp	Description
A	1	V t_{2g}
B	3	V t_{2g} ; O p_{π} ; O p_{σ}
C	4	V t_{2g} ; V e_g ; O p_{π} ; O p_{σ}

One of the reasons could be the lack of 4d orbitals in the impurity.

Coupled cluster could be used as an impurity solver.

Coupled cluster method

Wave function ansatz: $|\Psi\rangle = e^T |\Phi_0\rangle$; $T = \sum_{i,a} t_i^a a_a^\dagger a_i + \frac{1}{4} \sum_{i,j,a,b} t_{ij}^{ab} a_a^\dagger a_b^\dagger a_j a_i$

Amplitude equation: $\langle \chi_l | \bar{H} | \Phi_0 \rangle = 0$; $\bar{H} = e^{-T} H e^T$

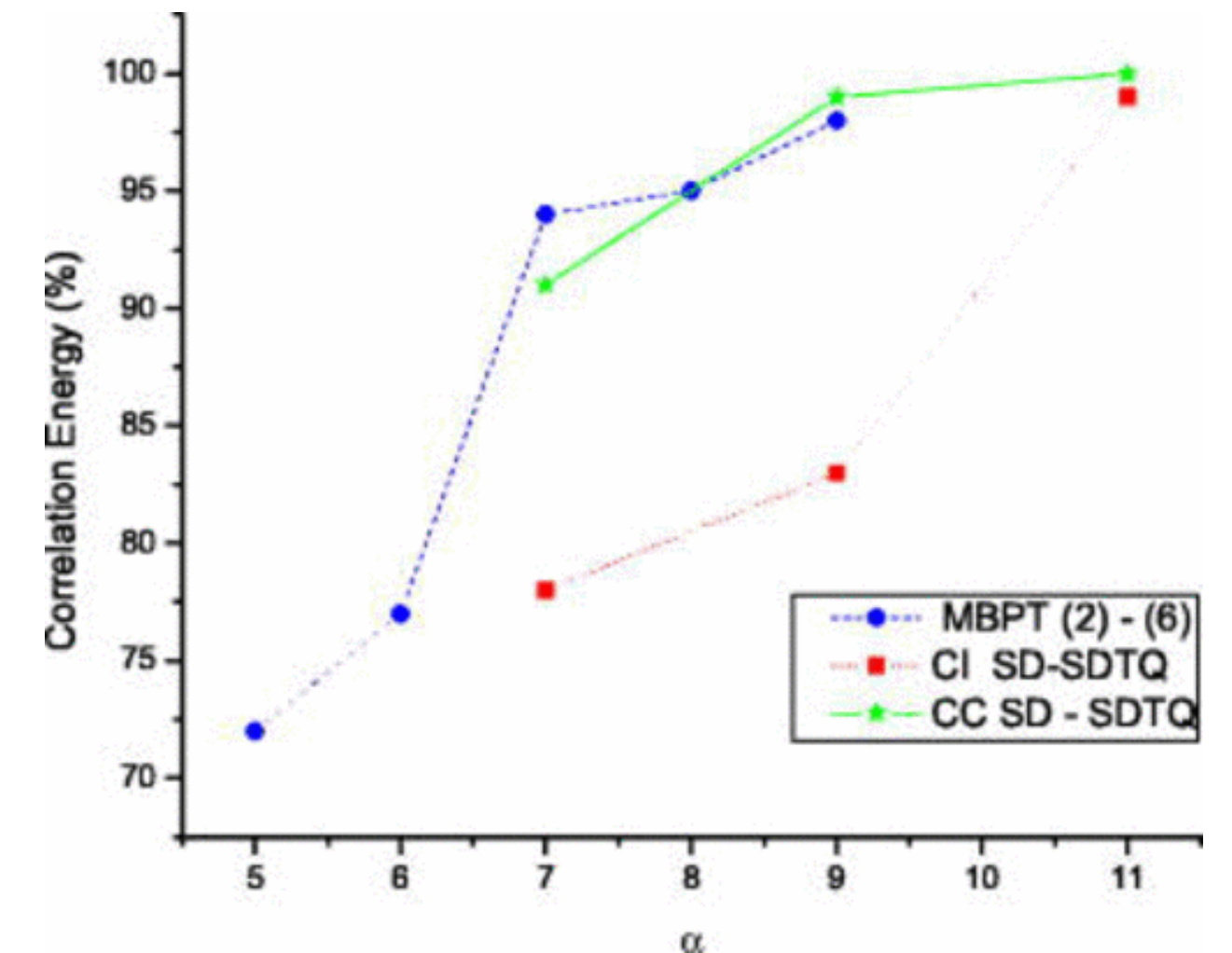
Energy equation: $E = \langle \Phi_0 | \bar{H} | \Phi_0 \rangle$

CI expansion: $|\Psi\rangle = (T_1 + T_2 + \dots + T_n) |\Phi_0\rangle$

-Includes all order perturbative terms of low-rank excitations.

-More compact than CI.

Coupled cluster considers more classes of diagrams: ring, exchange (absent in GW), ladder (absent in GW and GF2)



CC converges faster w.r.t. truncation

Definition of CCGF

Spectral representation:

$$G_{pq}(\omega) = \langle \Psi | a_p^\dagger \frac{1}{\omega + \mu + (H - E_{gr}) - i\eta} a_q | \Psi \rangle + \langle \Phi_0 | (1 + \Lambda) e^{-T} \langle \Psi | a_p \frac{1}{\omega + \mu - (H - E_{gr}) + i\eta} a_q^\dagger | \Psi \rangle e^T | \Phi_0 \rangle$$

$$= G_{pq}^{(h)} + G_{pq}^{(p)}$$

$$G_{pq}^{CC}(\omega) = \langle \Phi_0 | (1 + \Lambda) \bar{a}_p^\dagger \frac{1}{\omega + \mu + \bar{H} - i\eta} \bar{a}_q | \Phi_0 \rangle + \langle \Phi_0 | (1 + \Lambda) \bar{a}_p \frac{1}{\omega + \mu - \bar{H} + i\eta} \bar{a}_q^\dagger | \Phi_0 \rangle,$$

$$\frac{1}{\omega + \mu + \bar{H} - i\eta} \bar{a}_q | \Phi_0 \rangle$$

Frequency dependent *Complex*

Complexity: $2N_\omega N^5$

#M. Nooijen and J. Snijders, Int. J. Quant. Chem. 55 (1992)

K. Bhaskaran-Nair, K. Kowalski, WA. Shelton, JCP 144, 144101 (2016)

Unstable around the poles in real frequency calculations.

CCGF continues...

For inversion we do Lanczos based tridiagonalization followed by continued fraction

$$T = P^T \bar{H} Q = \begin{pmatrix} \alpha_1 & \gamma_1 & 0 & \dots & 0 \\ \beta_1 & \alpha_2 & \gamma_2 & \dots & 0 \\ 0 & \beta_2 & \alpha_3 & \ddots & 0 \\ 0 & 0 & \ddots & \ddots & 0 \end{pmatrix}$$

$$G_{(N-1)}^{CC}(\omega) = \frac{N_{IP}}{(\omega + \mu - i\eta) + \alpha_0 - \cfrac{\gamma_0 \beta_0}{(\omega + \mu - i\eta) + \alpha_1 - \cfrac{\gamma_1 \beta_1}{(\omega + \mu - i\eta) + \alpha_2 - \dots}}}$$

Advantages over other formulations:

- Scaling is independent of N_ω
- Doesn't suffer from instability at specific frequency points.
- No complex response equations.

Further discussion of scaling of CCGF

N-particle problem scales as n^6

(N-1)/(N+1)-particle problem scales as n^5

G_{pq} consists of $n(n+1)/2$ number of (N-1)/(N+1)-particle problems. We parallelize over the number of elements:

```
total_num_tasks = Ns*(Ns+1)//2
max_processes = args.ccsdgf_procs if total_num_tasks >=args.ccsdgf_procs else total_num_tasks
task_size = total_num_tasks//max_processes
task_list = np.array([task_size]*max_processes)
for i in range(total_num_tasks % max_processes):
    task_list[i] += 1

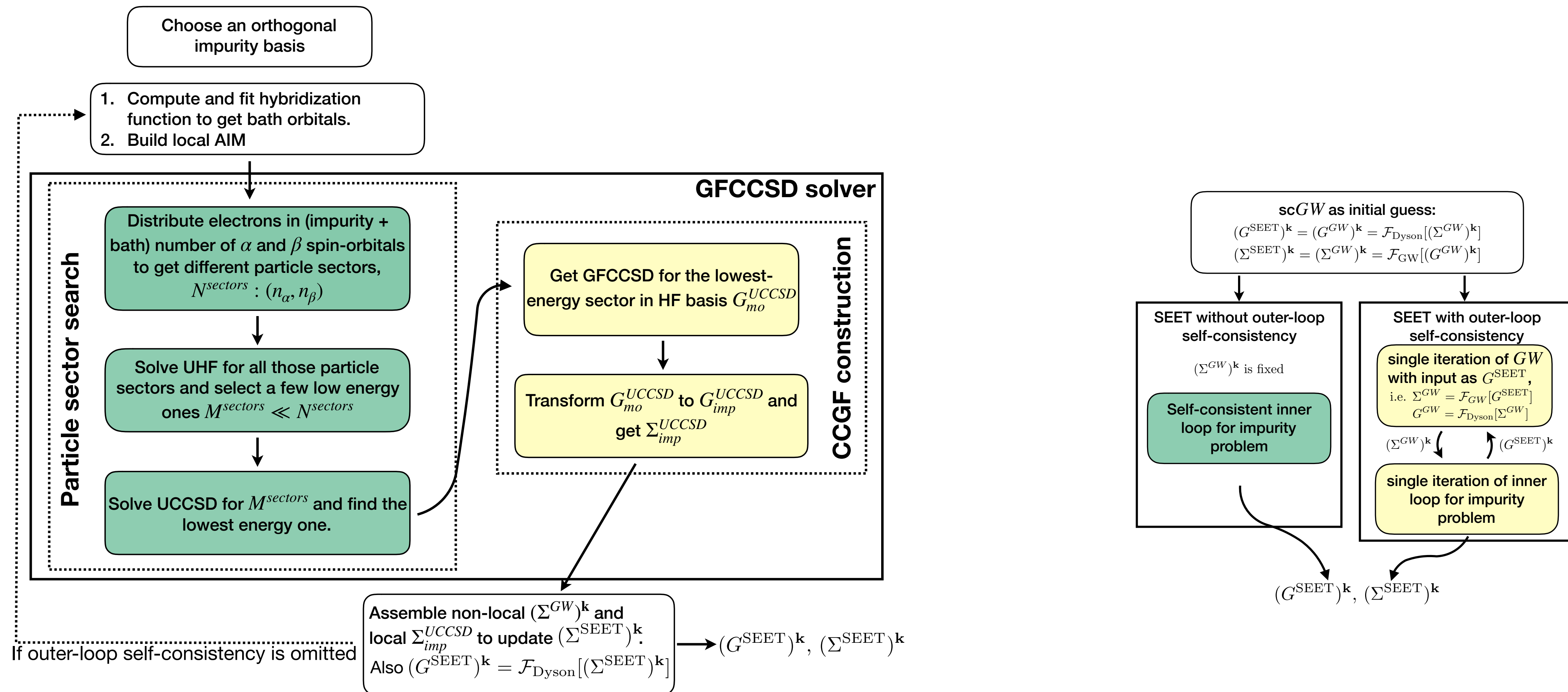
print("Calculating CCSD Green's function for impurity ", str(imp))
sys.stdout.flush()
calc_gf(iter, imp, Ns, nno, a, b, args.aquarius, task_list, nw, inv_T, args.cc_num_lanczos)
```

Using python multiprocessing module

Aquarius is mpi parallelized. But because of the single node requirement of python we can't take much advantage of it yet.

CCGF as a solver for SEET

SEET Schematic view

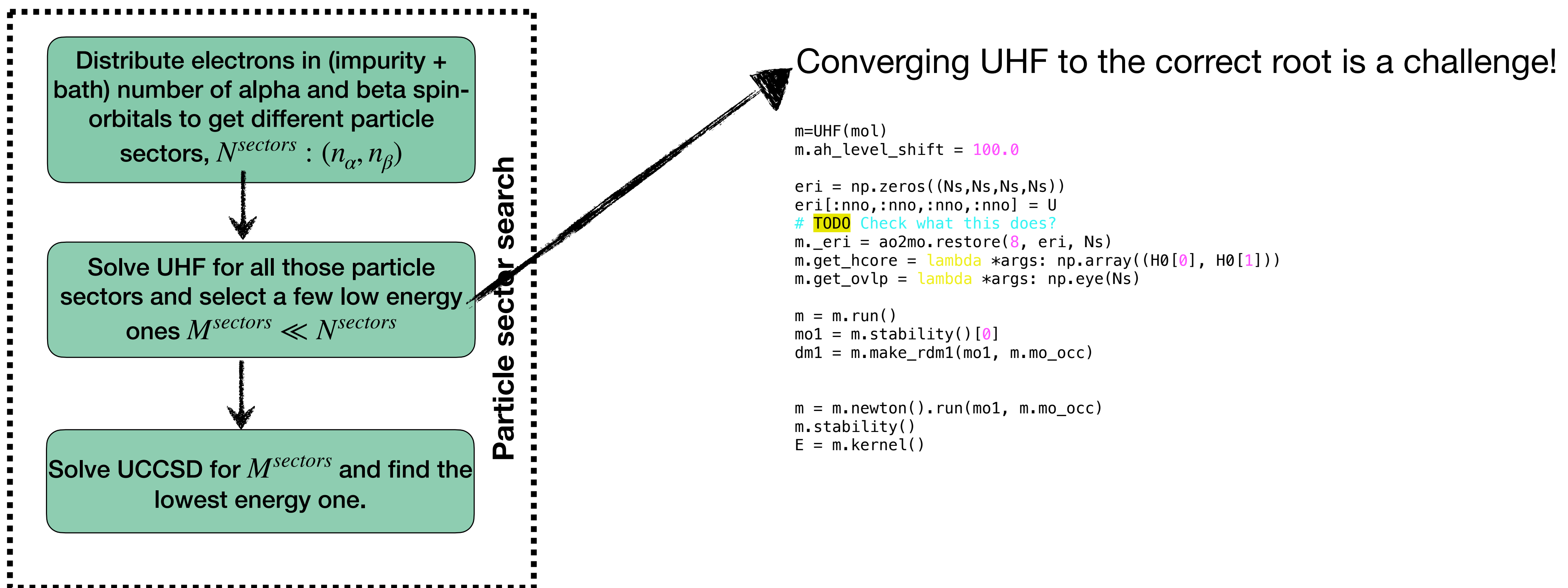


Particle sector search

Why it is important?

Correct chemical potential for the correlated problem is unknown

What we do:



Analysis of particle sector search

UHF	UCCSD	UCCSD(T)	ED
(9,6), (6,9) [-19.059]	(9,6), (6,9) [-19.083]	(8,7), (7,8) [-19.092]	(9,6), (6,9), (8,7), (7,8) [-19.086]
(9,7), (7,9) [-19.027]	(8,7), (7,8) [-19.073]	(9,6), (6,9) [-19.088]	(8,7), (7,8) [-19.043]
(8,7), (7,8) [-19.023]	(8,6), (6,8) [-19.031]	(8,6), (6,8) [-19.036]	(8,7), (7,8) [-19.041]

t_{2g} impurity of $SrMnO_3$

UHF	UCCSD	UCCSD(T)	ED
(8,5), (5,8), (6,8), (8,6) [-5.771]	(6,6) [-5.855]	(6,6) [-5.872]	(6,6) [-5.866]
(8,7), (7,8) [-5.765]	(7,6), (6,7) [-5.846]	(7,6), (6,7) [-5.861]	(7,6), (6,7) [-5.855]
(6,6) [-5.757]	(8,6), (6,8) [-5.839]	(7,7) [-5.849]	(6,5), (5,6) [-5.848]

P impurity of $SrMnO_3$

1. Unphysical mixing of spin sectors happen
2. UHF can predict a wrong particle sector.

We often restrict the search within a specific spin.

Total Energy based analysis of the particle sector

Total energy in the particle sector search is another good indicator of the accuracy of the solver.

Choice of impurities for the example of MnO:

A : $[\sigma_{Mn:3d_z^2+O:2p_z}, \sigma_{Mn:4s+3d_z^2+O:2p_z}^*, \delta_{Mn:3d_{xy}}]$,

B : $[p\pi_{Mn:3d_{xz}+O:2p_x}, d\pi_{Mn:3d_{xz}+O:2p_x}, \pi_{Mn:4p_x+O:4p_x}, d\pi_{Mn:4d_{xz}+O:4p_x}]$,

C : $[p\pi_{Mn:3d_{yz}+O:2p_y}, d\pi_{Mn:3d_{yz}+O:2p_y}, \pi_{Mn:4p_y+O:4p_y}, d\pi_{Mn:4d_{yz}+O:4p_y}]$

Table 5. Comparison of Correlation Energies in au for Various Impurities with an Increasing Rank of CC Theory for the MnO Molecule Using an Impurity Hamiltonian^a

imp	CCSD	CCSDT	CCSDTQ	ED
A	-0.009756	-0.009761	-0.009761	-0.009768
B	-0.017697	-0.017818	-0.017818	-0.017821
C	-0.017696	-0.017818	-0.017818	-0.017867
A + B + C	-0.150818	-0.167700	too costly due to size	too costly due to size

For A+B+C, SEET(GW/CCSD) fails to converge!!

1. Correlation energy gives an estimate of the convergence w.r.t. rank
2. Low rank truncation often insufficient if number of particles in an impurity is high.

Thermal Green's function?

$$G = \frac{\sum_k e^{-i\beta(\epsilon_k - \epsilon_0)} g_k}{\sum_k e^{-i\beta(\epsilon_k - \epsilon_0)}}$$

1. We need to evaluate g_k s for different particle sectors.
2. Both for ground and excited states of each of them.

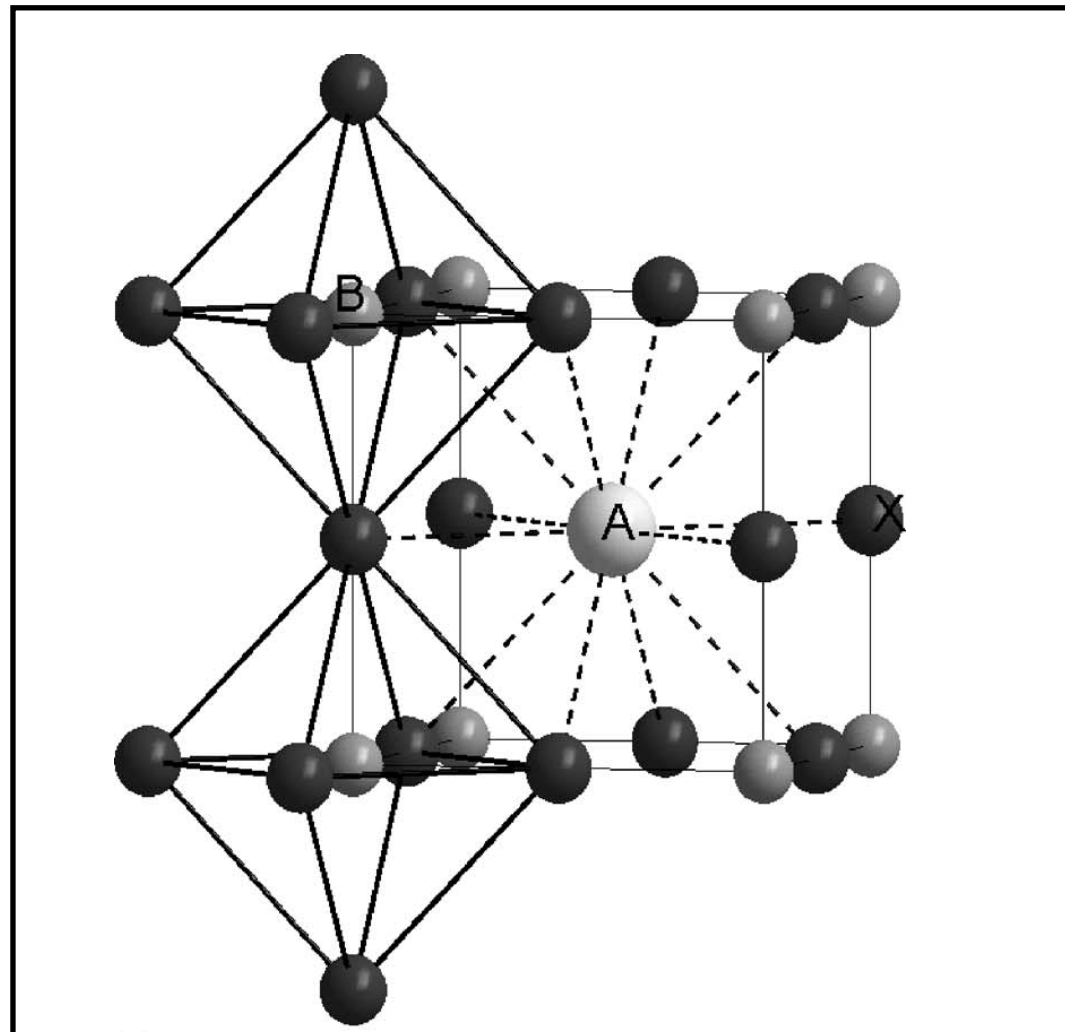
With coupled cluster we can evaluate only the ground state Green's function. This is a limitation of this formulation.

For spin-degenerate cases, we always employ the averaging, i.e., $(m_\alpha, n_\beta) + (n_\alpha, m_\beta)$

For other degenerate cases, it is not perfect. This can be a problem for metallic cases.

Whether CCSD truncation is sufficient?

Oxide Perovskite SrMnO_3



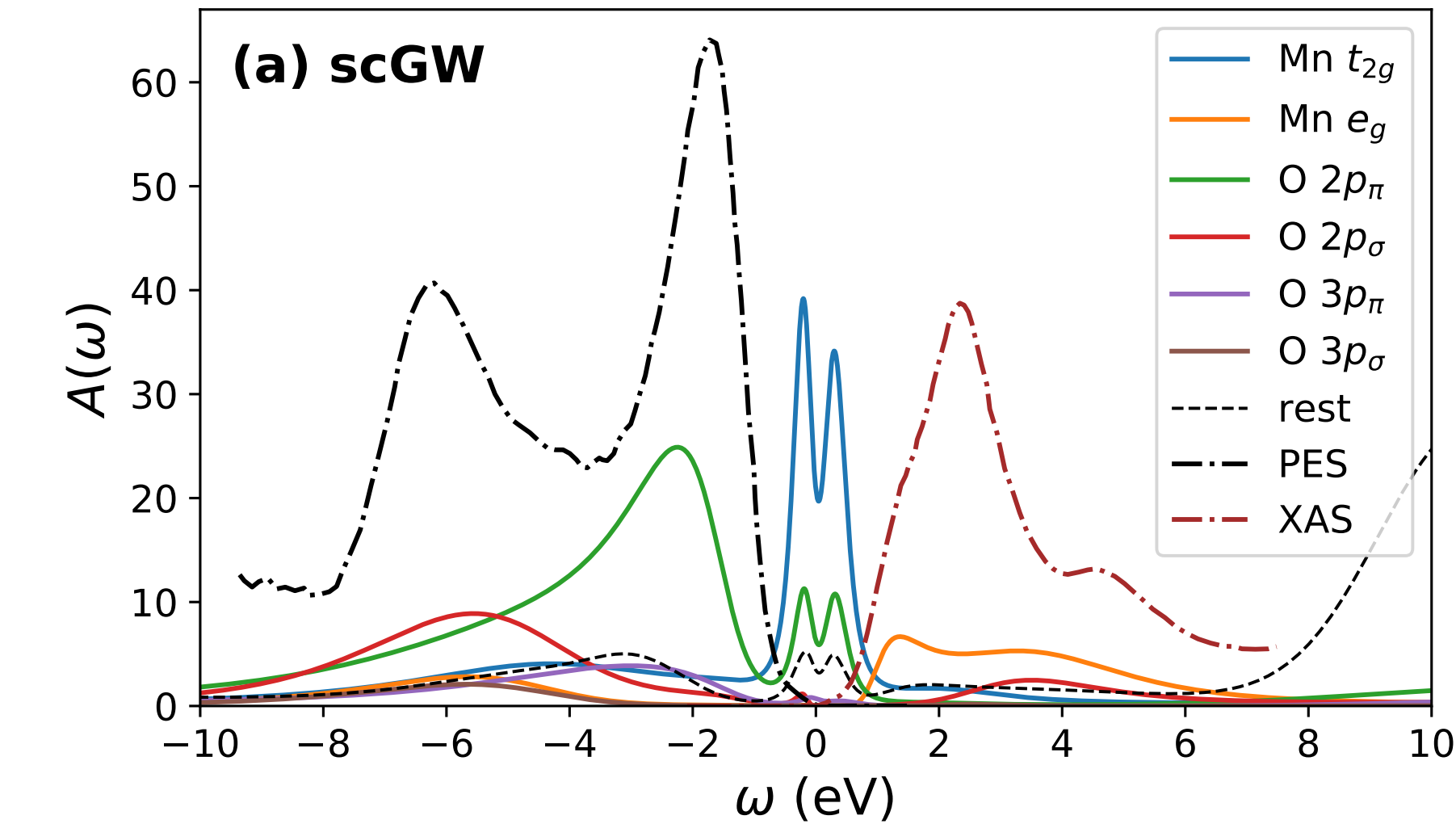
Cubic perovskite in paramagnetic phase
 $T = 1053 \text{ k}$

Experiment predicts a gap of 1.0-2.3 eV

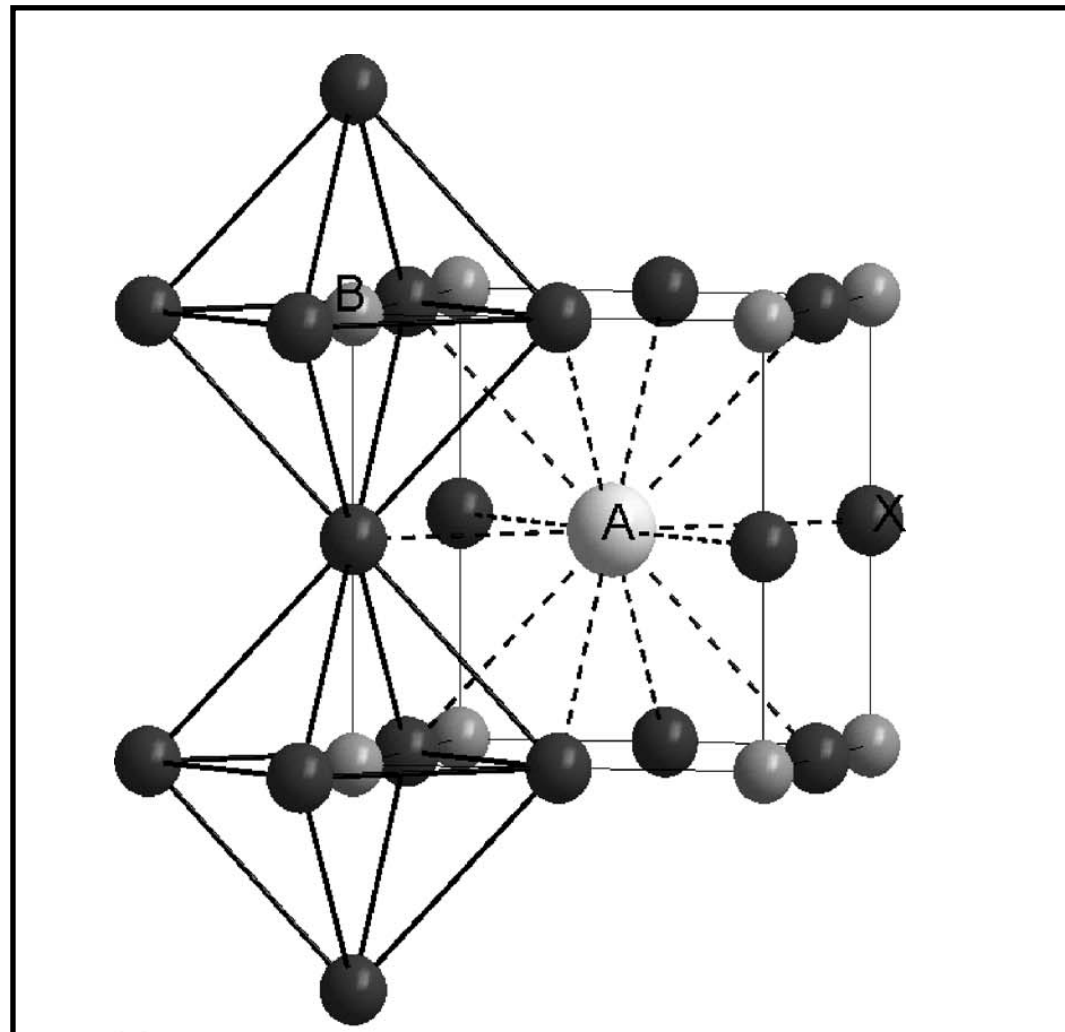
With SEET(GW/ED) we see gap opening¹. We want to investigate whether SEET (GW/CCSD)
Is also successful in that!!

Two different computational setups will be used:

- 1) Mn: t_{2g}
- 2) Mn: t_{2g} ; Mn: e_g ; O: p_π ; O: p_σ



Oxide Perovskite SrMnO_3

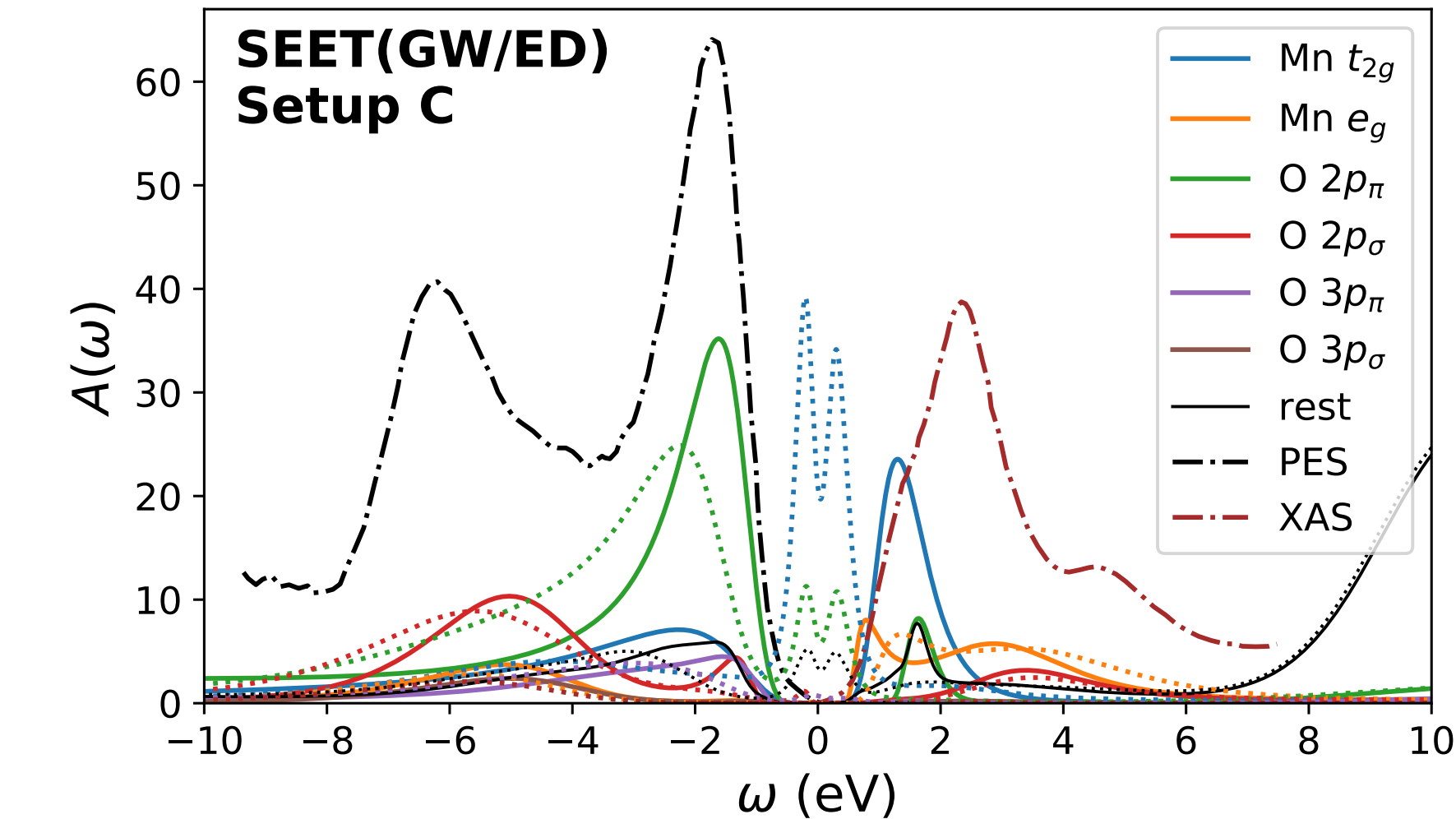


Cubic perovskite in paramagnetic phase
 $T = 1053 \text{ K}$

With SEET(GW/ED) we see gap opening¹. We want to investigate whether SEET (GW/CCSD) Is also successful in that!!

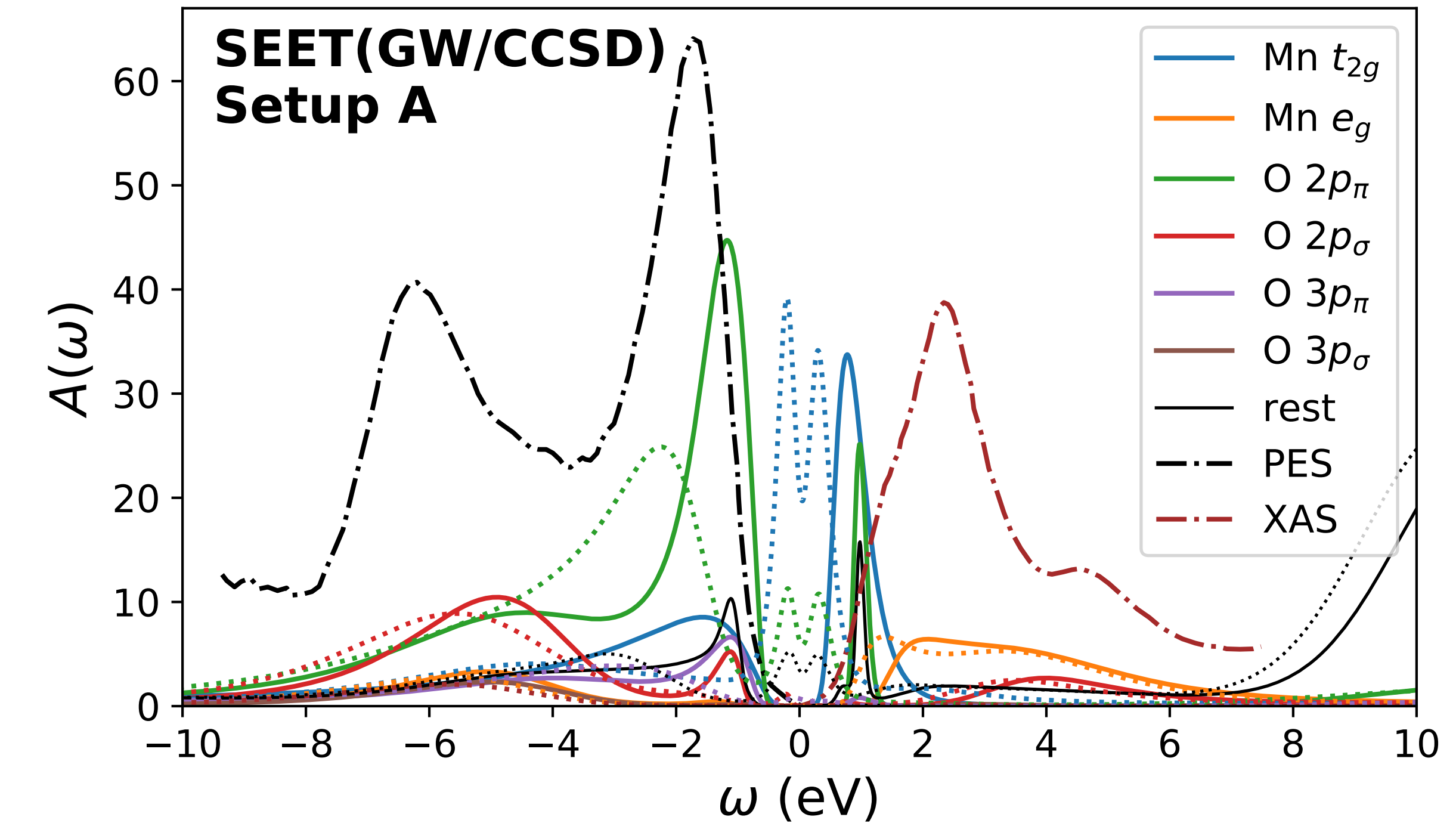
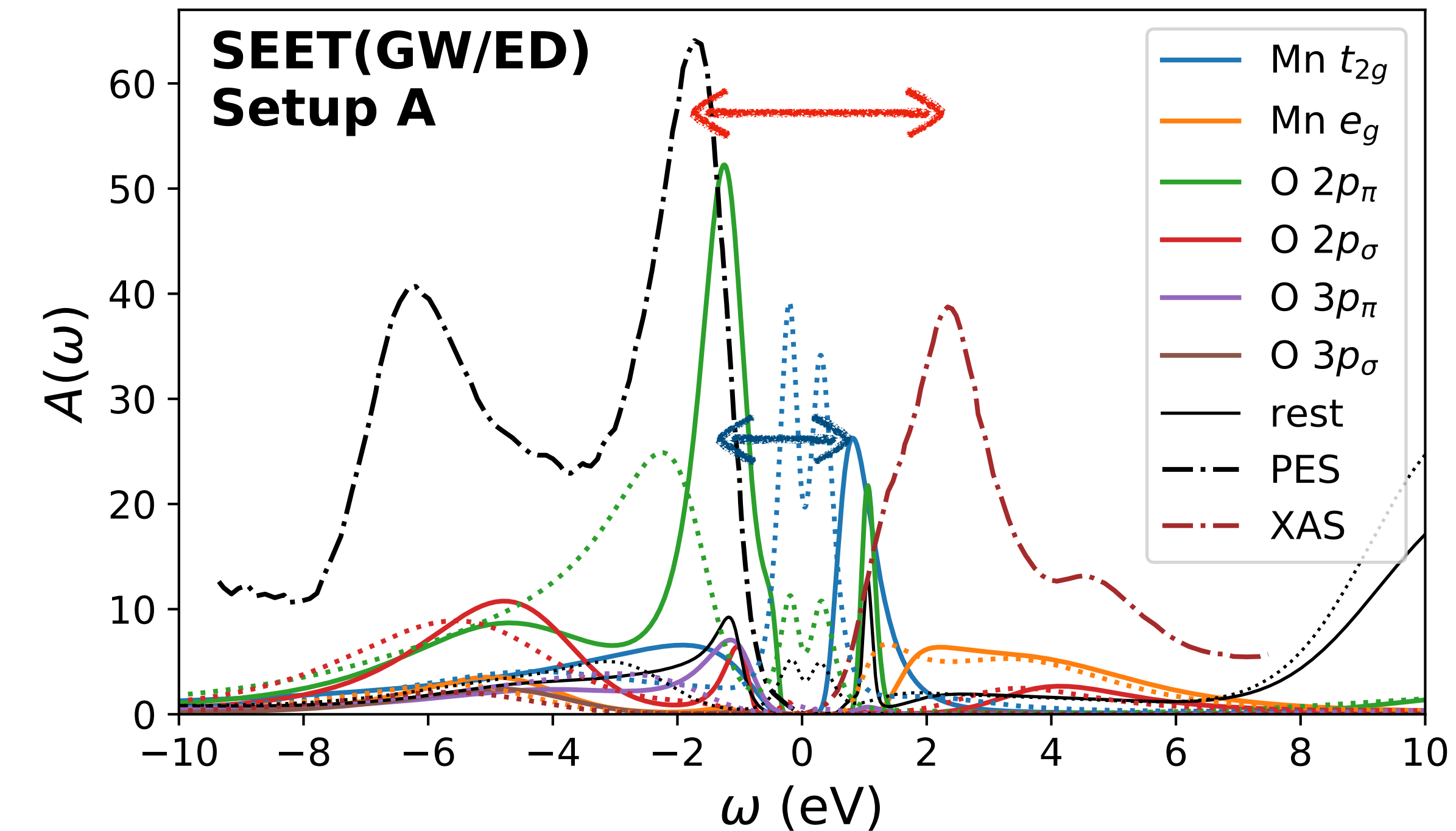
Two different computational setups will be used:

- 1) Mn: t_{2g}
- 2) Mn: t_{2g} ; Mn: e_g ; O: p_π ; O: p_σ



DOS comparison

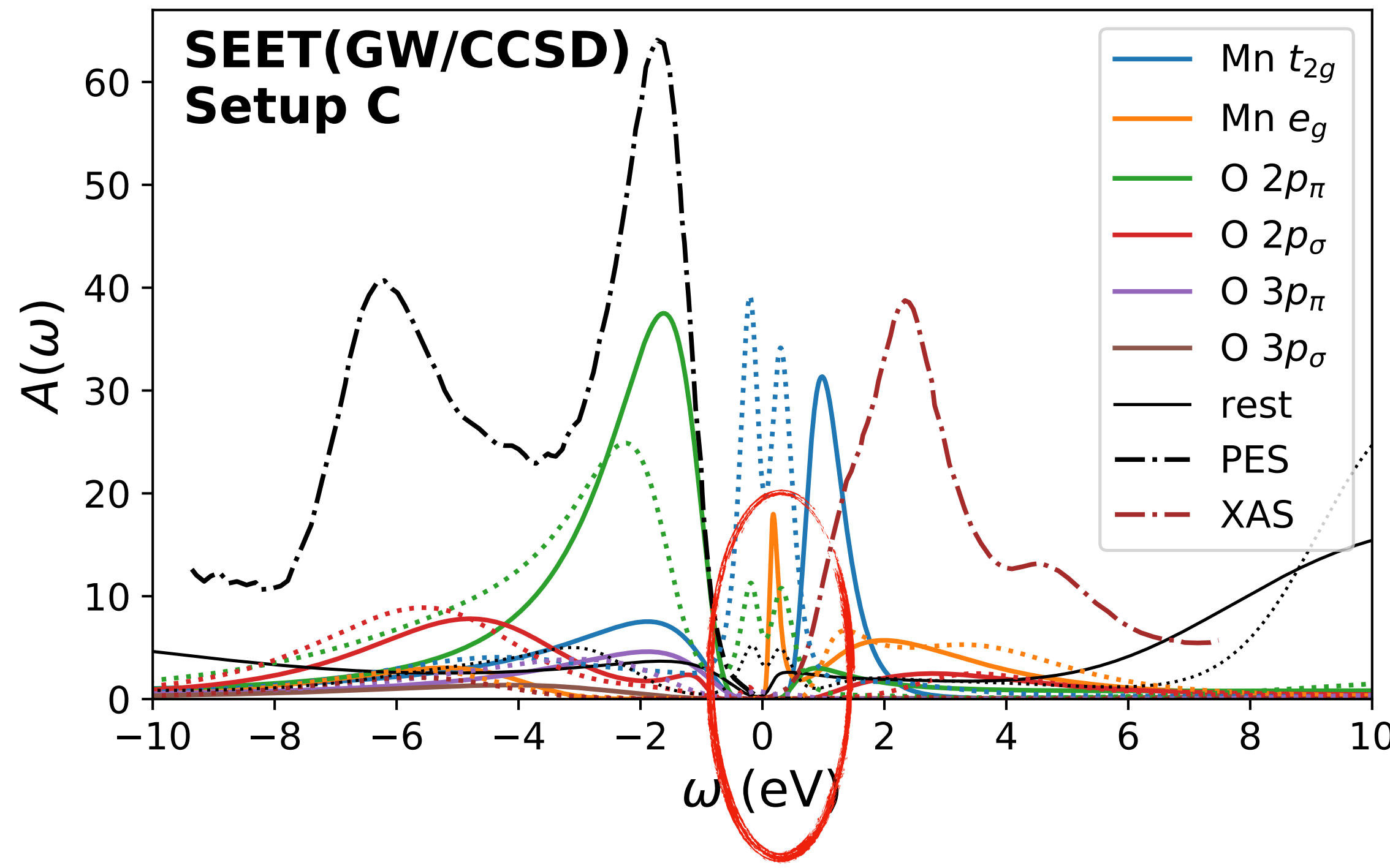
After carrying out both inner and outer loop self-consistency



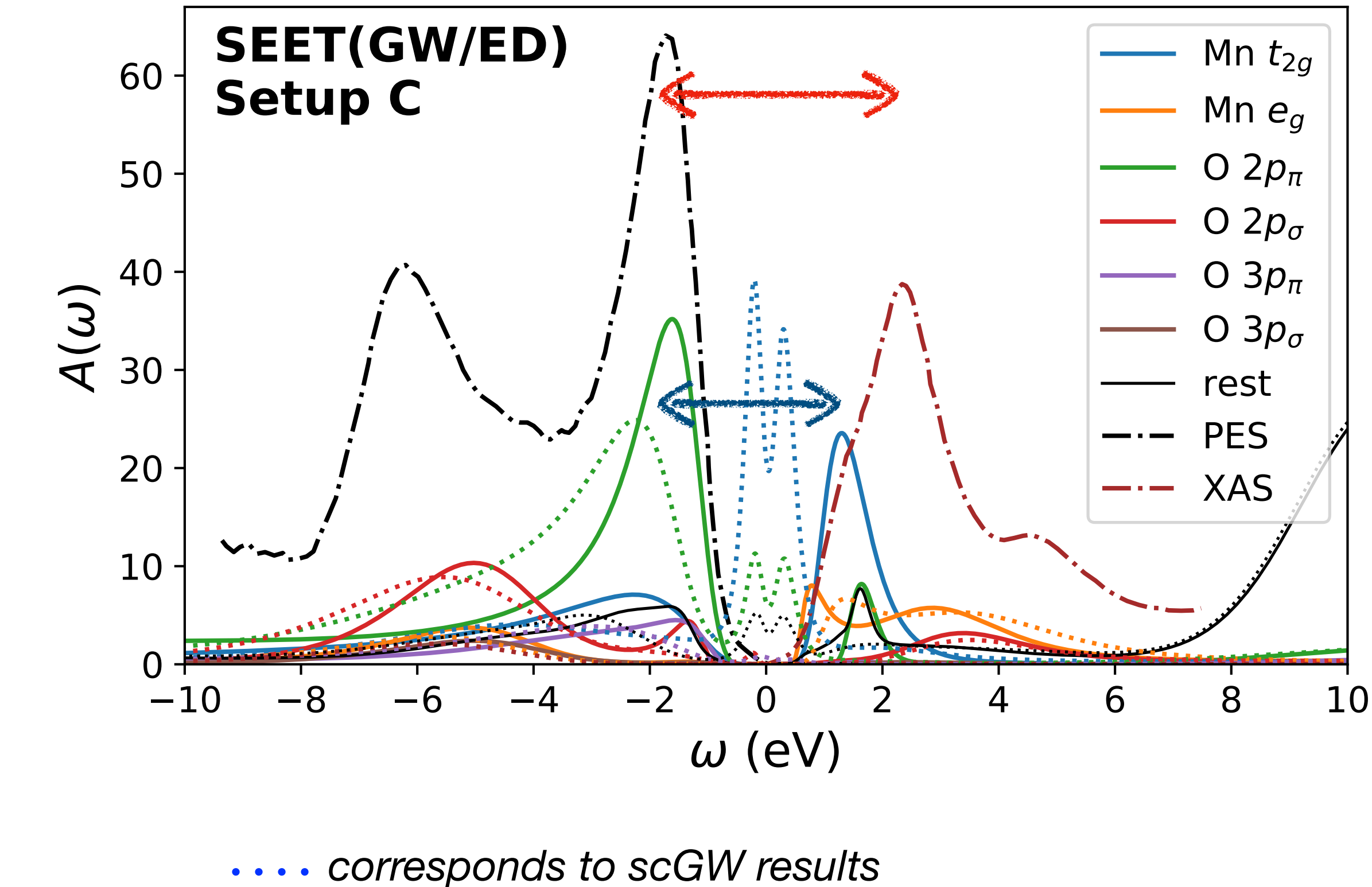
..... corresponds to scGW results

Setup A: Mn: t_{2g}

DOS comparison (Mn: t_{2g} + e_g)



Spurious e_g peak near E_F



We have to improve the GFCC solver.

GFCCSDT solver and approximation

Theory

Full GFCCSDT scales as N^8 . We are looking for a slightly cheaper variant.

$$|\Psi_{gr}\rangle = e^{\hat{T}} |\Phi_0\rangle; \quad \hat{T} = \hat{T}_1 + \hat{T}_2 + \hat{X}_3$$

$$|\Psi_{N+1/N-1}\rangle = e^{\hat{T}} \hat{R}_{N+1/N-1} |\Phi_0\rangle$$

$$\hat{R} = \hat{R}_1 + \hat{R}_2 + \hat{R}_3$$

GFCCSDT(2,3) variant scales as N^7

$$G_{ij} = \sum_k \frac{X_{ik}^\dagger X_{ki}}{\omega + E_G - E_k + i\eta} X_{ik} = \langle GS | c_i^\dagger | E_k \rangle \rightarrow \text{More complete projection of (N-1) states..}$$

The GFCCSDT(2,3) approximation is free of disconnected diagrams (B. Peng and K. Kowalski) for (N+1)/(N-1) cases.

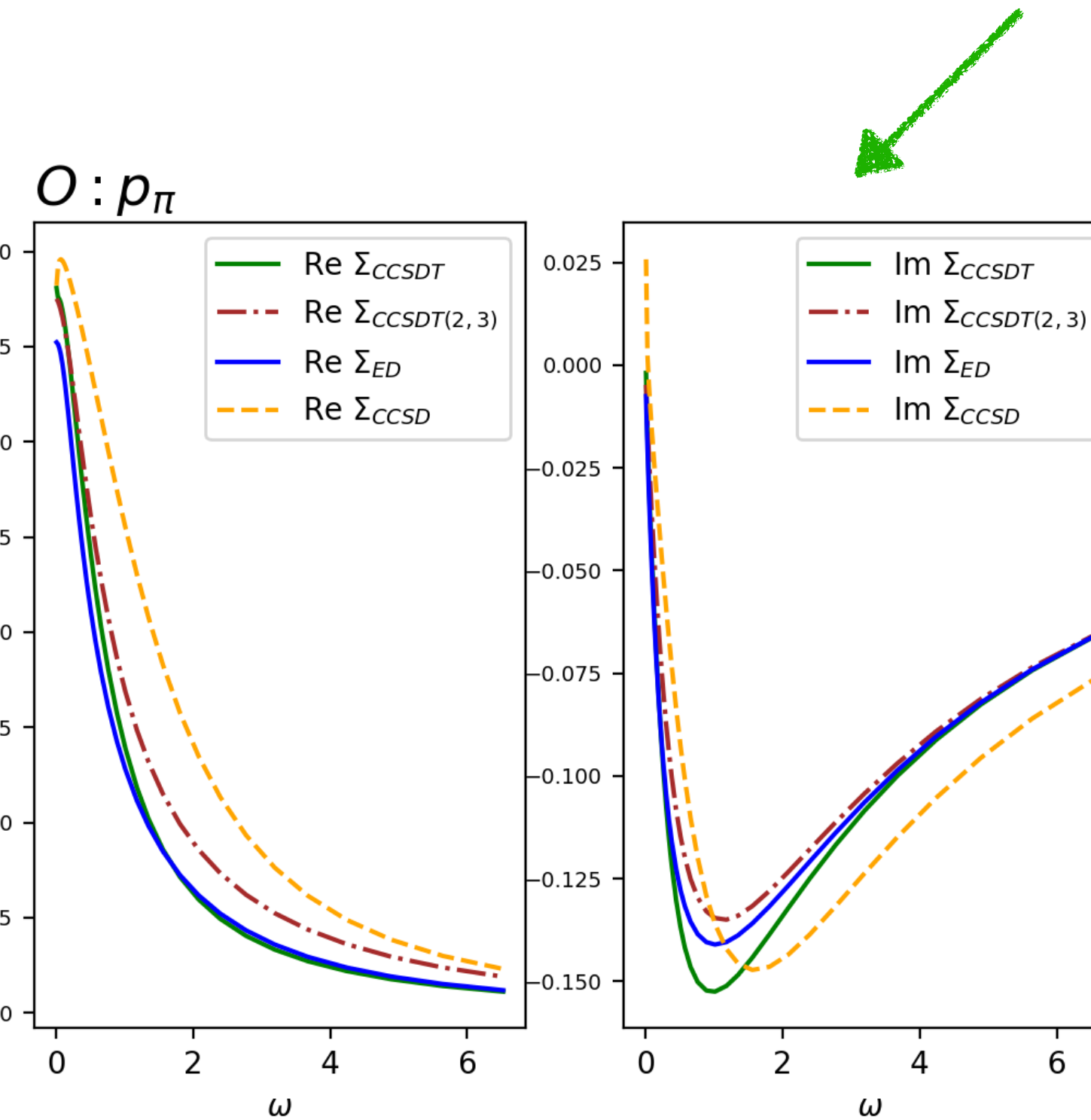
System	EOM-CCSD poles	GFCCSDT(2,3) poles
Singly-excited electronic states	0.1-0.2 eV	0.01
Doubly-excited electronic states	≥ 1 eV	0.1-0.2
Severe spin-contamination of the reference	~ 0.5 eV	≤ 0.1
Breaking single bond (EOM-SF)	0.1-0.2 eV	0.01
Breaking double bond (EOM-2SF)	~ 1 eV	0.1-0.2

Table 6.3: Performance of the EOM-CCSD and EOM-CC(2,3) method

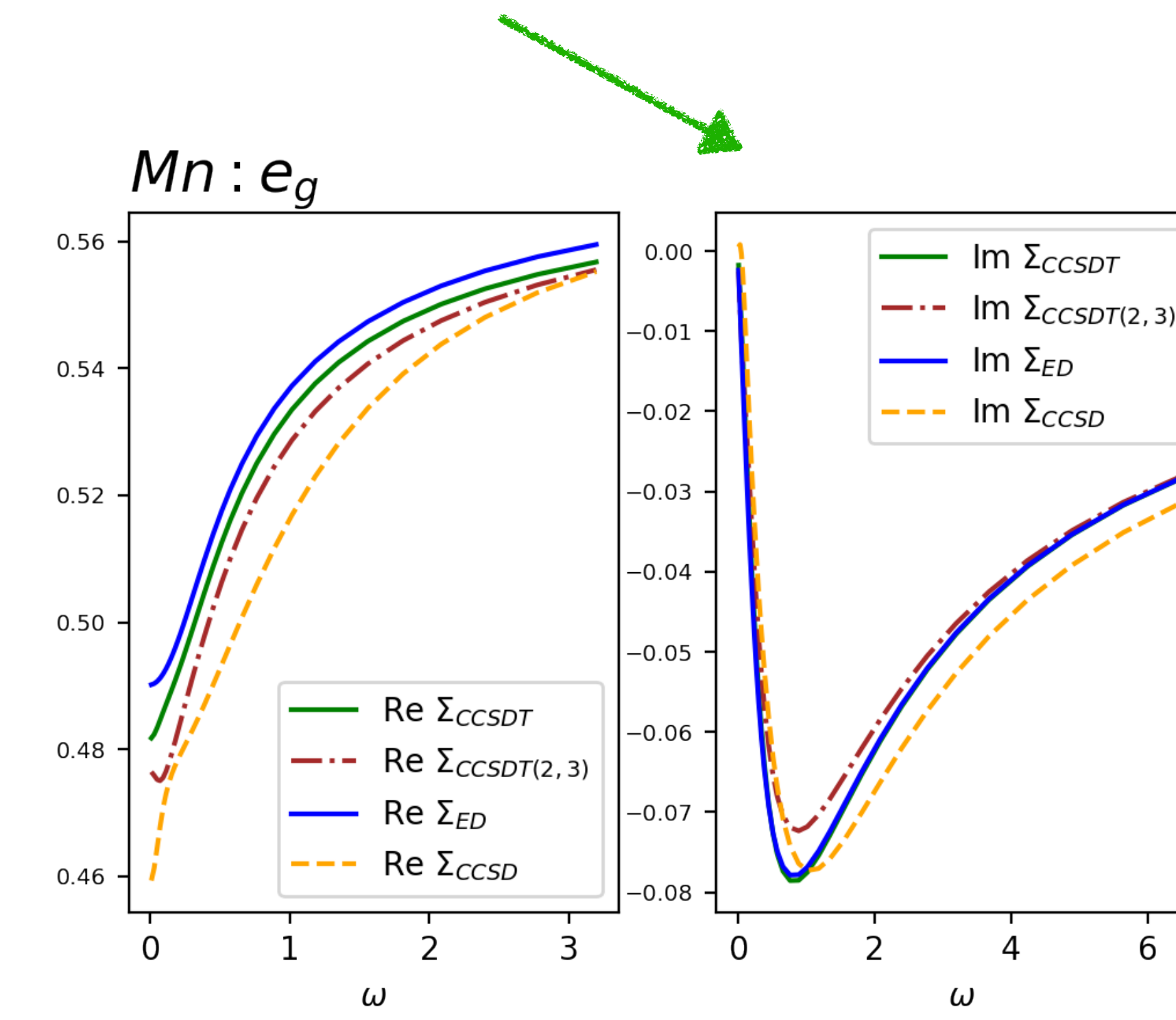
Source: Q-Chem manual

Self-energy comparison : $Mn : e_g$ and $O : p_\pi$

No causality breakdown anymore!!



$O:p_\pi$ impurity



$Mn: e_g$ impurity

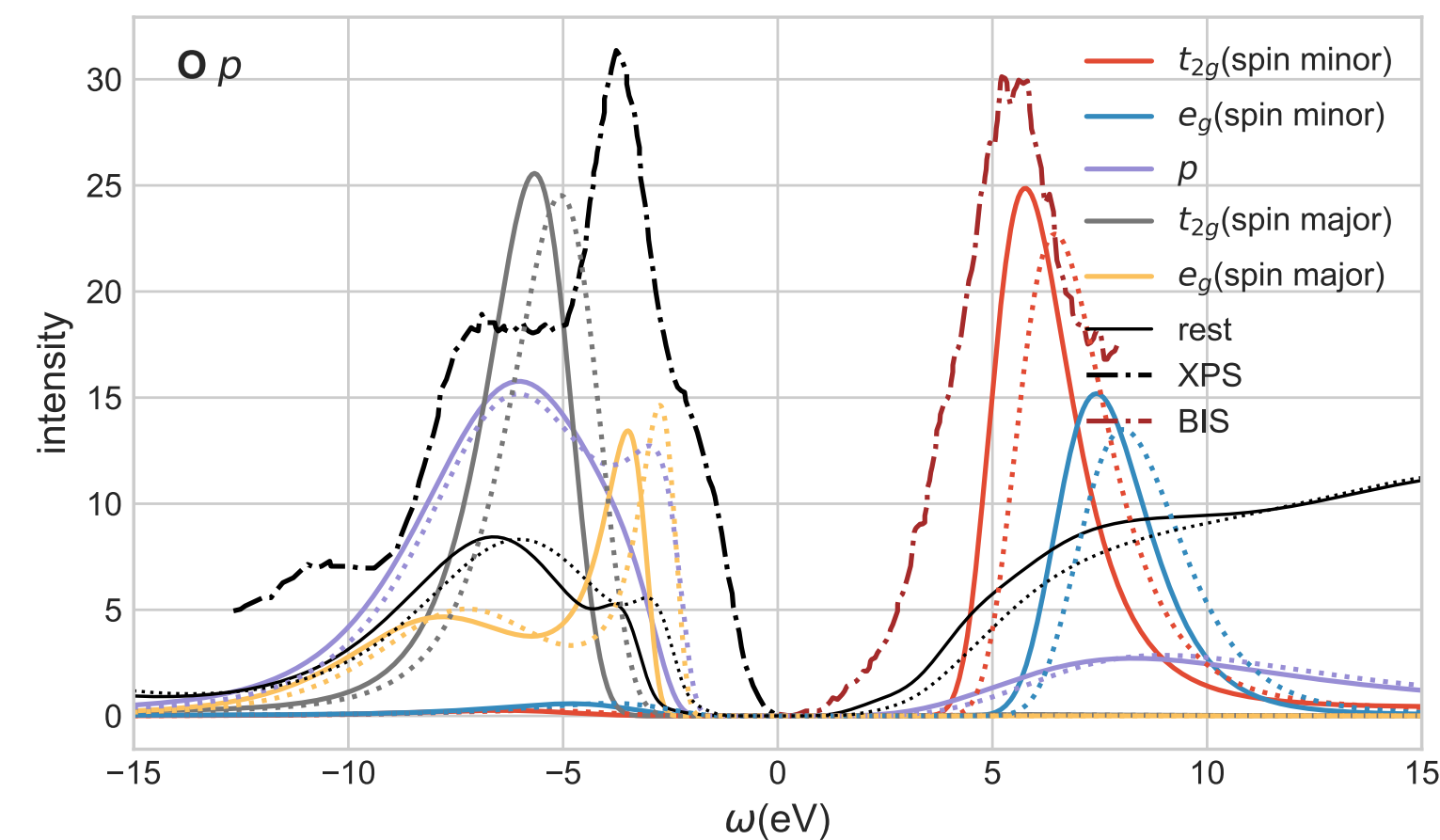
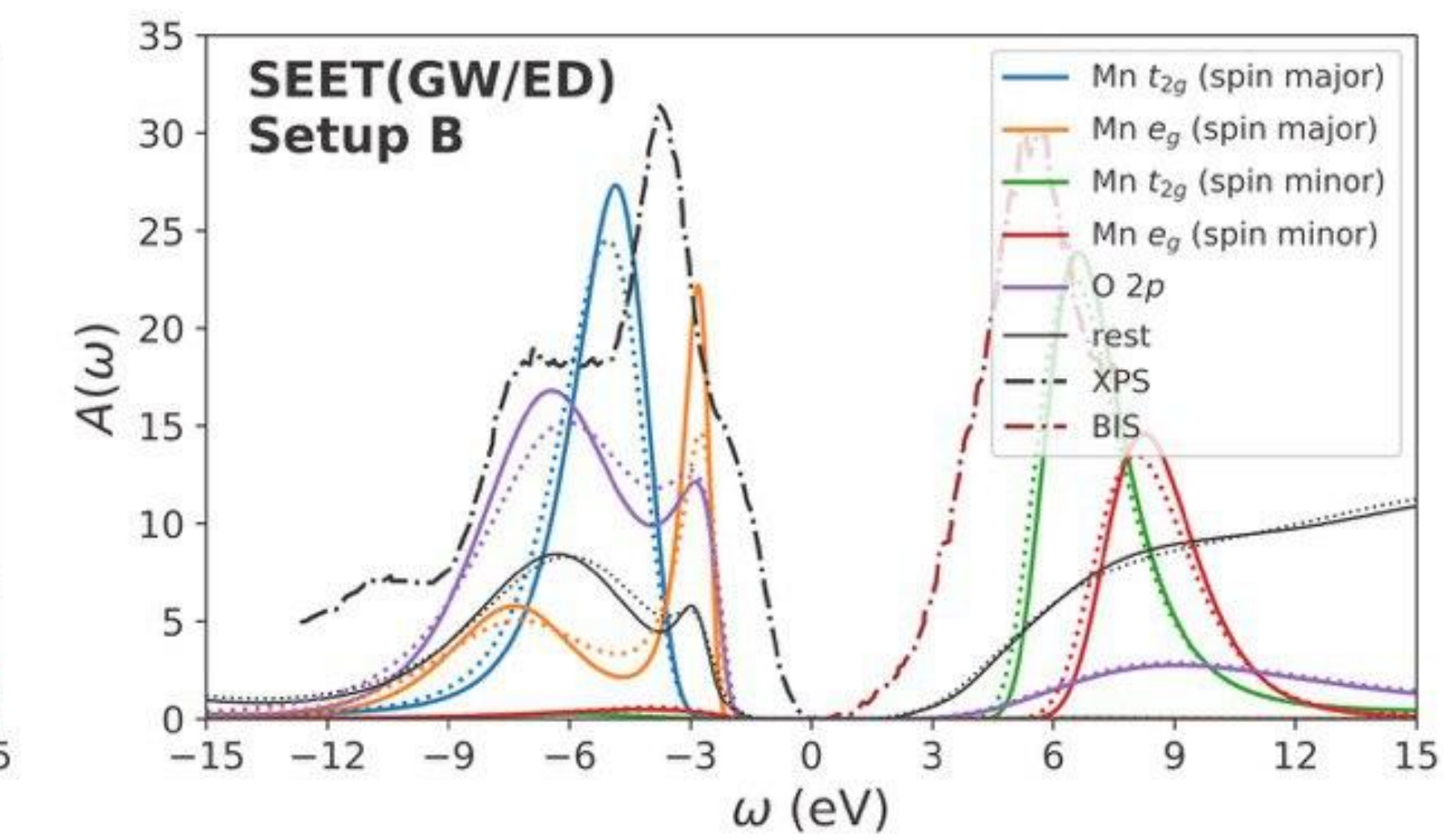
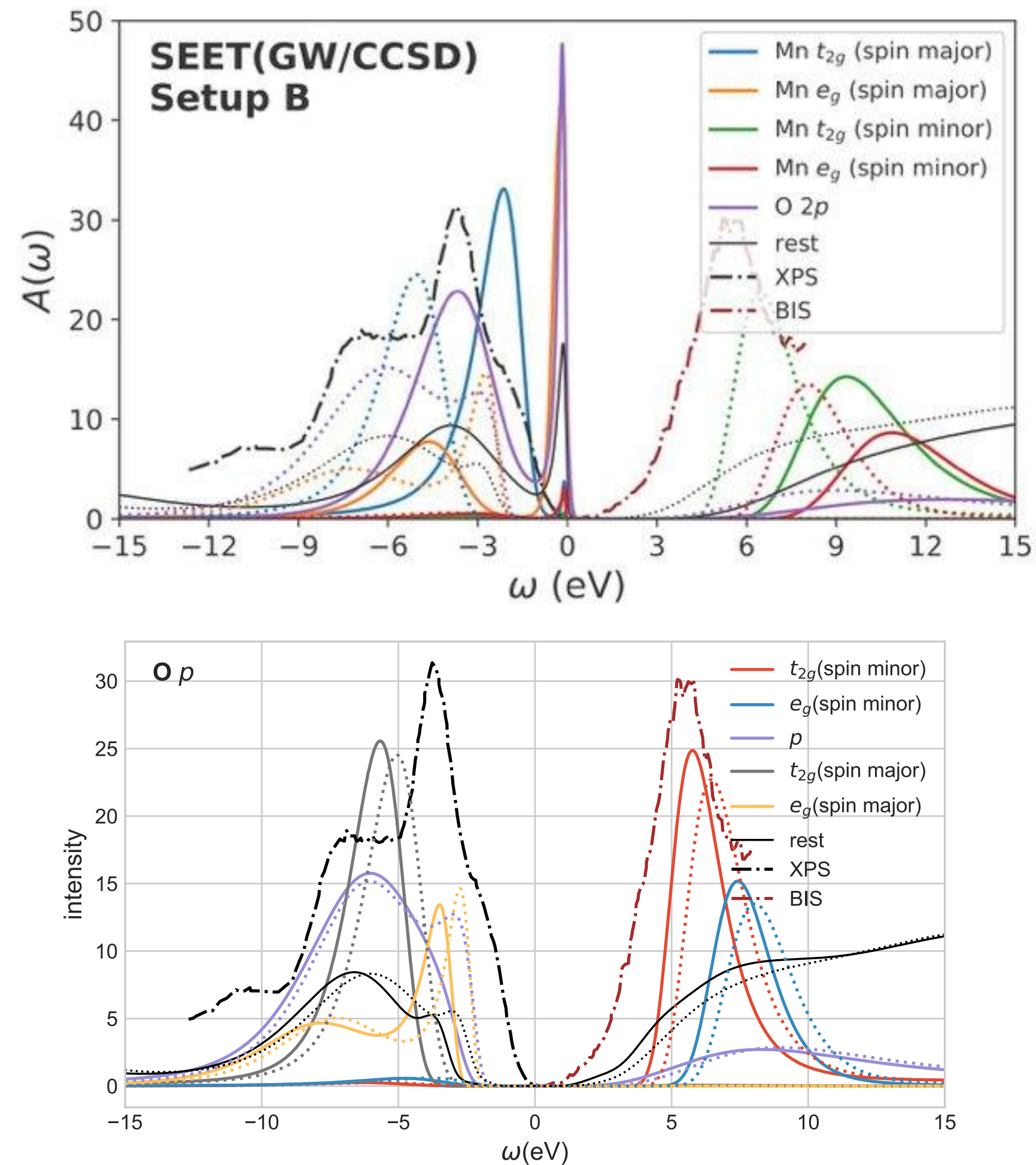
Self-consistency test with MnO:

$Mn : t_{2g}, e_g; O : p_\pi + p_\sigma$

We have chosen AFM Phase of MnO for this investigation.

-MnO doesn't require the charge self-consistency loop.

-GFCCSD produces a spurious peak at E_F when O:p is the impurity.



SEET(GW/CCSDT(2,3))

Final Remarks

1. Lanczos based CCGF is numerically efficient and stable.
2. Error in particle sector search may lead to divergence in SEET
3. With increasing size of the impurity accuracy deteriorates.
4. GFCCSDT provides significant improvement over GFCCSD.